Temperature Dependence of Polyolefin Melt Rheology

H. MAVRIDIS *and* R. N. SHROFF

Quantum Chemical Corp., USI Division
Allen Research Center
Cincinnati, Ohio 45249

The rheology of polymer melts depends strongly on temperature. Quantifying this temperature dependence is very important for fundamental, as well as practical, reasons. The purpose of this paper is to present a unified framework for handling the temperature dependence of rheological data. We considered the case (by far the most common in polymer melts) where all relaxation times (in the context of linear viscoelasticity) have the same temperature dependence (characterized by a "horizontal shift activation energy") and all relaxation moduli have the same temperature dependence (characterized by a "vertical shift activation energy"). The horizontal and vertical activation energies were extracted from loss tangent vs. frequency and loss tangent vs. complex modulus data, respectively. This is the recommended method of calculation, as it allows independent estimation of the two activation energies (statistically uncorrelated). It was shown theoretically, and demonstrated experimentally, that neglect of the vertical shift leads to a stress (or modulus) dependent activation energy and necessitates different activation energies for the superposition of loss and storage modulus data. The long standing problem of a stress-dependent activation energy in long chain branched LDPE was identified as originating from the neglect of the vertical shift. The theory was applied successfully to many polyolefin melts, including HDPE, LLDPE, PP, EVOH, LDPE, and EVA. Linear polymers (HDPE, LLDPE, PP) and EVOH do not require a vertical shift, but long chain branched polymers do (LDPE, EVA). Steady-shear viscosity data can be superimposed using activation energies extracted from dynamic data.

INTRODUCTION

Temperature has a significant effect on the rheological properties of polymer melts. Quantification of this dependence is important for several reasons. First, it eliminates the need for rheological measurements at multiple temperatures. Measuring rheological data at one temperature and knowing the temperature dependence parameters (activation energies in the nomenclature of this paper) is all we need to predict the rheological response at any other temperature. An example drawn from industrial practice is given in the **Appendix**.

A second major reason for establishing the temperature dependence of rheology relates to resin characterization. The rheology of polymer melts depends on temperature and on the underlying molecular structure (molecular weight and molecular weight distribution, long chain branching). When characterizing the rheology of a given resin we need to know how to separate the various effects. For example, Han and Lem (1) and Harrel and Nakajima (2) discuss the connection between molecular structure and rheology, and how the temperature effect is to be blocked out in such a correlation.

The temperature dependence of rheology needs also to be quantified and modeled appropriately for all computer simulation work, including screw extrusion simulations, coextrusion simulations, and general die flow computations.

Finally, the temperature dependence of rheology is of importance to fundamental studies on the mechanism of flow of polymer melts. For example, it turns out that the flow activation energy of linear low density polyethylene (LLDPE) with octene as a comonomer is higher than that of an LLDPE with butene as a comonomer (as will be shown and discussed later in this paper). Long chain branched LDPE shows an even higher activation energy, plus some other anomalies (a stress-dependent activation energy when data are shifted at constant stress).

The purpose of this paper is to develop a unified framework to treat both dynamic and steady rheological data and apply it to polyolefin melts.

TEMPERATURE DEPENDENCE OF RHEOLOGY

Background

The temperature dependence of rheology has mainly been discussed in the literature either in the context of linear viscoelasticity or in terms of steady-shear viscosity. In the latter case the shear stress σ, the shear rate $\dot{\gamma}$, and the viscosity η, are related through:

$$\sigma = \eta \cdot \dot{\gamma} \tag{1}$$

Mendelson (3) showed how to extract the temperature dependence from steady shear viscosity data by plotting the shear stress (vertical) vs. the shear rate (horizontal) data at different temperatures.

A review of the literature shows that it was established early on that polymer melts are thermorheologically simple. According to Markovitz (4), the term "thermorheological simplicity" was originated by Schwarzl and Staverman (5) as the "assumption of uniform temperature dependence for all relaxation elements." The modulus is usually only weakly dependent on temperature (6), and thus thermorheological simplicity has come to signify the ability to superpose data from different temperatures by a horizontal shift on a shear stress vs. shear rate graph (for steady shear data) or on a modulus vs. frequency graph (for linear viscoelastic data). The temperature shift is expressed in terms of a flow activation energy for polyolefin melts. When the flow activation energy shows a stress dependence (for stress vs. shear rate data) or a modulus dependence (for modulus vs. frequency data), then this is characterized as "thermorheological complexity." Long chain branched polyethylene (LDPE) exhibits thermorheological complexity (in contrast to the behavior of linear polyethylenes) as was pointed out repeatedly in the literature (7–13).

It will be shown in this paper that LDPE may still be considered "thermorheologically simple" in the sense that all relaxation times have the same temperature dependence and all relaxation moduli have the same temperature dependence (characterized by a "vertical" or modulus temperature shift). However, neglect of the "vertical" or modulus shift leads to a modulus (or stress) dependent flow activation energy, and thus to an *apparent* thermorheological complexity.

Early experimental observations that: (a) long chain branched polyethylene (LDPE) has a higher flow activation energy than linear polyethylene (HDPE), and (b) the flow activation energy of LDPE depends on shear stress (for shear stress vs. shear rate data, shifted horizontally) were reported by Sabia (7) and Mendelson (8). Porter and co-workers (9, 14, 15) examined the effects of polymer composition and molecular structure on the flow activation energy of polymer melts and concluded that long chain branching in LDPE is responsible for the anomalous behavior of activation energy of LDPE. Similar observations and experimental confirmation of "thermorheological complexity" in LDPE have been reported repeatedly (9, 16–19).

Graessley and co-workers (10, 20–22) found indications of thermorheological complexity" in model branched polymer melts. Graessley (11, 12) examined theroetically the effect of long branches on the temperature dependence of rheology and suggested two reasons for the observed behavior. One has to do with the temperature dependence of the entanglement density; the other is related to the differences in the paths of conformational relaxation of linear and branched chains. Linear chains rearrange by reptation. The presence of long branches blocks reptation; the long chain branches themselves rearrange by passing through relatively compact conformational states that may have different energies, depending on the temperature coefficient of chain dimension in the species (12).

Verser and Maxwell (19) examined the temperature dependence of linear viscoelastic data (frequency response). They found that when the classical treatment of time-temperature superposition (6) was applied to the data, then the resulting activation energy was modulus dependent (in fact their data show the activation energy to increase with complex modulus, *Fig. 19* in Ref. 19, an unusual result for LDPE). The modulus dependence was removed when a modulus shift was also applied to the data ("vertical" as well as "horizontal" shift). Verser and Maxwell (19) obtained the vertical shift from the temperature dependence of the steady-state compliance. However, most commercial polyethylenes are so broad that the terminal region (i.e., the low frequency region where $G' \propto \omega^2$, $G'' \propto \omega$, and $J_e^o = G'/G''^2$) is not accessible and therefore the steady-state compliance J_e^o would have to be calculated through data extrapolation, which may introduce large errors. It is an objective of the present paper to develop procedures for obtaining the vertical shift from data available over the experimentally accessible range (thus not involving any extrapolation).

In what follows we will deal mainly with the temperature dependence of linear viscoelastic data for two reasons: (i) the steady shear data should have the same temperature dependence as the linear viscoelastic data (4), and (ii) linear viscoelastic data include both the viscous and the elastic response of the material and are therefore more complete. (Steady shear data usually involve the viscous response only. The elastic response, i.e., normal stresses, is very difficult to measure.)

The temperature dependence of linear viscoelastic data is usually discussed in terms of the relaxation spectrum $H(\tau)$, where $H(\tau)$ is the relaxation strength of the material at relaxation time τ. All other linear viscoelastic properties can be derived from the relaxation spectrum. For completeness and ease of refer-

ence we summarize the most common of them below:

Storage Modulus:

$$G'(\omega) = \int_{-\infty}^{+\infty} H(\tau) \frac{(\omega\tau)^2}{1+(\omega\tau)^2}\, d\ln\tau \qquad (2.1)$$

Loss Modulus:

$$G''(\omega) = \int_{-\infty}^{+\infty} H(\tau) \frac{(\omega\tau)}{1+(\omega\tau)^2}\, d\ln\tau \qquad (2.2)$$

Complex Modulus:

$$G^*(\omega) = \sqrt{G'(\omega)^2 + G''(\omega)^2} \qquad (2.3)$$

Complex Viscosity:

$$\eta^*(\omega) = \frac{G^*(\omega)}{\omega} \qquad (2.4)$$

Dynamic Viscosity:

$$\eta'(\omega) = \frac{G''(\omega)}{\omega} \qquad (2.5)$$

Loss Tangent:

$$\tan\delta(\omega) = \frac{G''(\omega)}{G'(\omega)} \qquad (2.6)$$

Certain other rheological properties are also derivable from the above functions:

Plateau Modulus:

$$G_N^o = \int_{-\infty}^{+\infty} H(\tau)\, d\ln\tau = \lim_{\omega\to\infty} G'(\omega) \qquad (3.1)$$

Zero-Shear Viscosity:

$$\eta_o = \int_{-\infty}^{+\infty} H(\tau)\tau\, d\ln\tau = \lim_{\omega\to 0} \eta^*(\omega) \qquad (3.2)$$

Compliance:

$$J_e^o = \frac{\int_{-\infty}^{+\infty} H(\tau)\tau^2\, d\ln\tau}{\left[\int_{-\infty}^{+\infty} H(\tau)\tau\, d\ln\tau\right]^2} = \lim_{\omega\to 0} \frac{G'(\omega)}{\eta_o^2\omega^2} = \lim_{\omega\to 0} \frac{G'(\omega)}{G''(\omega)^2} \qquad (3.3)$$

In the above ω is the frequency in units of rad/s.

Let us now discuss the temperature dependence of the linear viscoelastic spectrum. The fundamental assumption is that relaxation spectra derived from data at different temperatures can be made to superimpose by vertical (along the relaxation strength axis) and horizontal (along the time axis) shifts, (4):

$$b_T H(\tau/\alpha_T, T) = H(\tau, T_o) \qquad (4)$$

where α_T and b_T are the horizontal and vertical shift factors respectively, T is the temperature, and T_o is a reference temperature. The horizontal shift factor α_T reflects essentially the temperature dependence of relaxation time:

$$\tau(T) = \tau(T_o)\cdot\alpha_T \qquad (5)$$

while the vertical shift factor b_T reflects the temperature dependence of modulus

$$G_N^o(T) = G_N^o(T_o)/b_T \qquad (6)$$

where G_N^o is the plateau modulus as defined in *Eq 3.1*.

An early prediction for the temperature dependence of relaxation time was provided by the WLF equation (6):

$$\log_{10}(\alpha_T) = \frac{-17.4\cdot(T-T_o)}{51.6+T-T_o} \qquad (7)$$

The WLF equation holds in the range of temperatures from T_g to T_g + 100°C, where T_g is the glass transition temperature. For temperatures greater than T_g + 100°C, which is the processing range for polyolefin melts, the WLF equation is closely approximated by an Arrhenius-type equation:

$$\alpha_T = \exp\left[\frac{E_H}{R}\left(\frac{1}{T+273} - \frac{1}{T_o+273}\right)\right] \qquad (8)$$

where E_H is the horizontal shift activation energy and
R is the gas constant (1.987 cal/mole/°C). *Equation 8* is the form employed in the present work for the horizontal shift factor, as it is the appropriate form for polyolefin melts, and also because it only involves one parameter—the activation energy E_H.

The vertical shift factor will now be discussed in some detail. Dilute solution theories (6) predict that the modulus is proportional to the product of density and absolute temperature, which in turn suggests a shift factor:

$$b_T = \frac{\rho_o\cdot(T_o+273)}{\rho\cdot(T+273)} \qquad (9)$$

where ρ is the density and T is the temperature in degrees Celsius. The subscript "o" indicates reference conditions. The same result is predicted from the theory of rubber elasticity, which gives the following equation:

$$M_e = \frac{\rho\cdot R\cdot(T+273)}{G_N^o(T)} \qquad (10)$$

where M_e is the molecular weight between entanglements. On the assumption that the molecular weight between entanglements is independent of temperature, *Eq 10* directly yields *Eq 9*.

However, M_e may depend on temperature, and indeed this will be shown to be the case for long chain branched polyethylene. In that case the result of *Eq 9* does not hold, and the molecular weight between

entanglements varies as (from *Eqs 6* and *10*):

$$\frac{M_e(T)}{M_e(T_o)} = \frac{b_T}{\left[\frac{\rho_o \cdot (T_o + 273)}{\rho \cdot (T + 273)}\right]} \tag{11}$$

As will be shown below, there is no reason to fix *a priori* the vertical shift factor (as dictated above by the theory of rubber elasticity). The appropriate vertical shift factor can be extracted from the data along with the horizontal shift factor. For that purpose we will define a general form for the vertical shift factor, analogous to that for the horizontal shift factor involving a "vertical activation energy":

$$b_T = \exp\left[\frac{E_V}{R}\left(\frac{1}{T+273} - \frac{1}{T_o+273}\right)\right] \tag{12}$$

where E_V is the vertical activation energy.

Temperature Shifts of Linear Viscoelastic Data

To summarize the results of the previous section, we assume that the relaxation spectra from different temperatures can be made to superimpose according to *Eq 4*, i.e. using a horizontal, α_T, and a vertical, b_T, shift factor. The functional forms of the shift factors are given in *Eqs 8* and *12*, and they involve two parameters: the horizontal, E_H, and the vertical, E_V, activation energies.

The storage and loss moduli shift with temperature as:

$$b_T G'(\alpha_T \omega, T) = G'(\omega, T_o) \tag{13.1}$$

$$b_T G''(\alpha_T \omega, T) = G''(\omega, T_o) \tag{13.2}$$

From the above we see that the loss tangent shifts as:

$$\tan\delta(\alpha_T \omega, T) = \tan\delta(\omega, T_o) \tag{14}$$

i.e., the loss tangent remains invariant under a temperature shift. Therefore, it is convenient to redefine the various viscoelastic properties in terms of the loss tangent and temperature:

$$G'(T, \tan\delta) = \frac{1}{b_T} G'(T_o, \tan\delta) \tag{15.1}$$

$$G''(T, \tan\delta) = \frac{1}{b_T} G''(T_o, \tan\delta) \tag{15.2}$$

$$\omega(T, \tan\delta) = \frac{1}{\alpha_T} \omega(T_o, \tan\delta) \tag{15.3}$$

$$G^*(T, \tan\delta) = \frac{1}{b_T} G^*(T_o, \tan\delta) \tag{15.4}$$

$$\eta^*(T, \tan\delta) = \frac{\alpha_T}{b_T} \eta^*(T_o, \tan\delta) \tag{15.5}$$

Note that *Eqs 15.1–3* indicate that the crossover modulus G_c ($G_c(T) = G'(T, \tan\delta = 1) = G''(T, \tan\delta = 1)$) and crossover frequency ω_c ($\omega_c(T) = \omega(T, \tan\delta = 1)$) are convenient scaling parameters (selecting a modulus and frequency values at another arbitrary level of loss tangent provides equally acceptable scaling parameters), i.e. plotting G'/G_c or G''/G_c vs. ω/ω_c results in a temperature independent graph.

The temperature dependence of some commonly referred to viscoelastic properties is given by:

Plateau Modulus:

$$\frac{G_N^o(T)}{G_N^o(T_o)} = \frac{1}{b_T} \tag{16.1}$$

Zero-Shear Viscosity:

$$\frac{\eta_o(T)}{\eta_o(T_o)} = \frac{\alpha_T}{b_T} \tag{16.2}$$

Compliance:

$$\frac{J_e^o(T)}{J_e^o(T_o)} = b_T \tag{16.3}$$

Calculation of Activation Energies

The calculation of the activation energies will be based on the equations derived in the previous section. The important point to note is, from *Eq 15.3* we observe that plotting data from different temperatures as frequency vs. loss tangent (or vice versa) should give parallel curves separated by a certain distance determined by the horizontal shift factor α_T only (the vertical shift factor does not appear in this graph). Therefore, a frequency vs. loss tangent graph is ideally suited for the estimation of the horizontal activation energy E_H, since the estimation can be performed independently from that of the vertical activation energy E_V.

Similarly, from *Eq 15.4* we observe that plotting data from different temperatures as complex modulus, G^*, vs. loss tangent (or vice versa) should give parallel curves separated by a certain distance determined by the vertical shift factor b_T only (the horizontal shift factor does not appear in this graph).

The above observations justify the selection of dynamic data for the determination of the temperature dependence of rheology. Dynamic data allow independent estimation of the vertical and horizontal activation energies. Note that for other types of linear viscoelastic data commonly employed (shear stress relaxation modulus data, $G(t)$ vs. time t, or creep compliance data, $J(t)$ vs. time t), as well as for steady-shear viscosity data, the two activation energies cannot be computed independently.

The estimation is performed through nonlinear least-squares fitting of the data, as explained below.

Estimation of Horizontal Activation E_H

Frequency vs. loss tangent data from different temperatures are least-squares fitted to the following

form:

$$\log_{10}(\tan\delta) = \sum_{k=0}^{k=m} c_k \cdot [\log_{10}(\alpha_T \cdot \omega)]^k \quad (17)$$

where α_T is given by *Eq 8*. m is the order of the fitting polynomial (usually 3) and (c_k, $k = 0, m$) are the polynomial coefficients. The nonlinear least-squares fit involves ($m + 2$) parameters; ($m + 1$) polynomial coefficients and the activation energy E_H. The fit provides an estimate of the activation energy E_H and its 95% confidence interval, $E_H \pm \Delta E_H$, where ($E_H - \Delta E_H$, $E_H + \Delta E_H$) is the 95% confidence interval (in a statistical sense, (23)).

Estimation of Vertical Activation Energy E_V

Complex modulus vs. loss tangent data from different temperatures are least-squares fitted to the following form:

$$\log_{10}(\tan\delta) = \sum_{k=0}^{k=m} d_k \cdot [\log_{10}(b_T \cdot G^*)]^k \quad (18)$$

where b_T is given by *Eq 12*. m is the order of the fitting polynomial (usually 3) and (d_k, $k = 0, m$) are the polynomial coefficients. The nonlinear least-squares fit involves ($m + 2$) parameters; ($m + 1$) polynomial coefficients and the activation energy E_V. The fit provides an estimate of the activation energy E_V and its 95% confidence interval, $E_V \pm \Delta E_V$.

Once the horizontal and vertical activation energies have been computed, the data from different temperatures can be shifted to the reference temperature T_o (using *Eqs 13–15*) for visual inspection of the goodness of superposition.

Comments on the Vertical Shift Factor

As was mentioned in the **Background** discussion, the vertical shift factor predicted by the theory of rubber elasticity, as well as by dilute solution theories, is given by *Eq 9*. This shift factor is usually very nearly unity and can often be neglected, i.e., the data can be shifted at constant stress (for shear stress vs. shear rate data) or constant modulus (for modulus vs. time or frequency data). A shift factor of $b_T = 1$ corresponds to a vertical activation energy of $E_V = 0$. Such a shift factor is indeed appropriate for most linear polymers (as will be shown later).

To examine the magnitude of vertical shift factor predicted by *Eq 9*, we select a HDPE, for which the melt density was determined as a function of temperature (24):

$$\rho = 0.8696 - 5.62 \cdot 10^{-4} \cdot T \quad (19)$$

where ρ is the density in g/cm^3, and T is the temperature in °C.

If the vertical shift factor is given by *Eq 9*, then the equivalent vertical activation energy can be computed from:

$$E_V = \frac{R \cdot \ln\left(\frac{\rho_o \cdot (T_o + 273)}{\rho \cdot (T + 273)}\right)}{\left[\frac{1}{T + 273} - \frac{1}{T_o + 273}\right]} \quad (20)$$

The vertical activation energy was computed from *Eq 20* for two cases: first, with the density given by *Eq 19* and, second, for a temperature independent density. The resulting vertical activation energy, when the density variation with temperature is taken into account, is about 0.6 kcal/mole in the range 150 to 230°C. When the density variation is neglected, the effective activation energy is about 0.92 kcal/mole, which is an order of magnitude smaller than that for the horizontal shift activation energy. The shift factor varies between 0.9 and 1.1 in the range 150 to 230°C, i.e. it varies by about ±10%, a level of variation that may fall within the limits of experimental error.

The vertical shift factor predicted by theory is very close to unity and, therefore, it can be neglected for the example discussed above. When the vertical shift factor is neglected for long chain branched LDPE, then anomalous results are observed: the computed (horizontal) activation energy depends on stress (or modulus) as explained below.

Stress Dependent Activation Energy of LDPE: An Explanation

We will show now that: shifting data horizontally only will generally introduce a stress (or modulus) dependence of the (horizontal) activation energy, which only disappears in the limit of zero vertical activation energy. For this purpose we will use the schematic shown in *Fig. 1*: frequency (or shear rate) is plotted on the horizontal axis, while modulus (or stress) is plotted on the vertical axis. The symbol "G^{sup}" may represent G', G'' or G^*. We assume that for the data to shift from temperature T to temperature T_o a vertical, b_T, and horizontal, α_T, shifts are necessary, as shown in *Fig. 1*. This shift is indicated by the path 1 → 2 → 3 in *Fig. 1*. Now let us consider a shift at constant modulus, as indicated by the path, 1 → 4, i.e., a horizontal shift only at constant level of modulus. Let $\alpha_{T,G}$ be the shift factor associated with this shift, and let us define a corresponding activation energy E^{sup} as:

$$\alpha_{T,G} = \exp\left[\frac{E^{sup}}{R}\left(\frac{1}{T + 273} - \frac{1}{T_o + 273}\right)\right] \quad (21)$$

From *Fig. 1* we observe that the following relationship holds:

$$G^{sup}(\alpha_{T,G}\omega, T_o) = \frac{1}{b_T} G^{sup}(\alpha_T \omega, T_o) \quad (22)$$

where α_T and b_T are given by *Eqs 8* and *12* respectively. Taking the logarithm of both sides of *Eq 22*

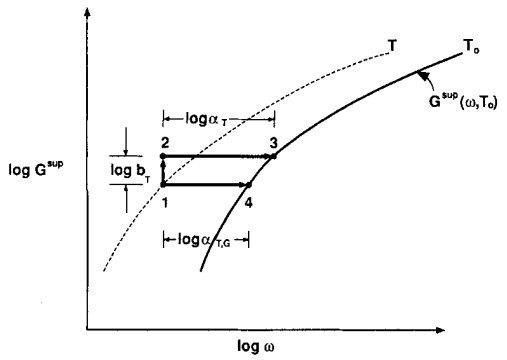

Fig. 1. Schematic of modulus vs. frequency at two temperatures, illustrating the two types of temperature shift; horizontal-only (1 → 4), and both vertical and horizontal shift (1 → 2 → 3).

and differentiating with respect to the inverse of absolute temperature we arrive at the following:

$$\frac{\partial \ln[G^{\sup}(\alpha_{T,G}\omega, T_o)]}{\partial \ln(\alpha_{T,G}\omega)} \cdot E^{\sup} = -E_V + \frac{\partial \ln[G^{\sup}(\alpha_T\omega, T_o)]}{\partial \ln(\alpha_T\omega)} \cdot E_H \Rightarrow E^{\sup}$$

$$= E_H \cdot \frac{\left[\dfrac{\partial \ln(G^{\sup}(\alpha_T\omega, T_o))}{\partial \ln(\alpha_T\omega)}\right]}{\left[\dfrac{\partial \ln(G^{\sup}(\alpha_{T,G}\omega, T_o))}{\partial \ln(\alpha_{T,G}\omega)}\right]} - E_V \cdot \frac{1}{\left[\dfrac{\partial \ln(G^{\sup}(\alpha_{T,G}\omega, T_o))}{\partial \ln(\alpha_{T,G}\omega)}\right]} \quad (23)$$

To simplify the above equation for the purposes of illustration, assume that over the range of frequencies $(\alpha_{T,G}\omega, \alpha_T\omega)$ the $G^{\sup}$ vs. ω curve can be approximated by a power-law form:

$$G^{\sup} \alpha\, \omega^n \Rightarrow \frac{\partial \ln G^{\sup}}{\partial \ln \omega} = n \quad (24)$$

where n is the power-law exponent. Substituting in *Eq 23*:

$$E^{\sup} = E_H - \frac{E_V}{n} \quad (25)$$

From *Eqs 22–25* we observe that:

(i) when $E_V = 0$, then $b_T = 1$, and $\alpha_{T,G} = \alpha_T$, which implies that $E^{\sup} = E_H$, i.e., when a vertical shift is not necessary then shifting the data at constant modulus will yield a constant activation energy, which is the horizontal activation energy.

(ii) when $E_V \neq 0$ then shifting the data at constant modulus will yield an activation energy $E^{\sup}$ that decreases with increasing modulus according to *Eq 25* (because the power-law exponent n decreases with increasing modulus). Moreover, *Eq 25* shows that in that case it is impossible to superimpose both the storage and loss modulus data with the same activation energy. To prove this, consider the variation with frequency in the terminal region:

$$\frac{\partial \ln[G'(\omega)]}{\partial \ln \omega} = 2, \quad \text{for } \omega \to 0 \quad (26.1)$$

$$\frac{\partial \ln[G''(\omega)]}{\partial \ln \omega} = 1, \quad \text{for } \omega \to 0 \quad (26.2)$$

and substituting in *Eq 23*:

$$E' = E_H - \frac{E_V}{2}, \quad \text{for } \omega \to 0 \quad (27.1)$$

$$E'' = E_H - E_V, \quad \text{for } \omega \to 0 \quad (27.2)$$

from *Eq 27* we observe that in the terminal region the superposition of the storage modulus data gives an activation energy E' which is different from the activation energy E'' required for superposition of the loss modulus data.

The conclusion, therefore, is that neglecting the vertical shift not only makes the activation energy a function of modulus but also necessitates different activation energies for the storage and loss modulus data.

It is now easily understandable why steady shear viscosity data for LDPE yield a shear stress-dependent activation energy: it is like the case of shifting data at constant loss modulus examined above. In fact if normal stress data were to also be shifted, then a different activation energy would have been found (much the same as shifting at constant storage modulus yields an E' different from E''). The above theoretical results will be further corroborated by the experimental data to be presented in later sections.

Temperature Shifts of Steady-Shear Data

The preceding discussion dealt with the temperature shifts of linear viscoelastic data. It can be shown, from fundamental considerations (4), that steady-shear data must be superposable with the same shift factors. If $\sigma(\dot\gamma, T)$ is the shear stress at shear rate $\dot\gamma$ and temperature T, then the superposition of the steady-shear data can be obtained with the following formula:

$$b_T \sigma(\alpha_T \dot\gamma, T) = \sigma(\dot\gamma, T_o) \quad (28)$$

which is the equivalent of *Eq 13* for steady-shear data, where α_T and b_T are the horizontal and vertical shift factors respectively.

If the horizontal and vertical activation energies are not available, they can still be extracted from the steady-shear data. The estimation can proceed similarly to that outlined for dynamic data, i.e. by least-squares fitting the data to the form:

$$\log_{10}(b_T \cdot \sigma) = \sum_{k=0}^{k=m} c_k \cdot [\log_{10}(\alpha_T \cdot \dot\gamma)]^k \quad (29)$$

where α_T is given by *Eq 8*, b_T is given by *Eq 12*, m is the order of the fitting polynomial, and (c_k, $k = 0, m$) are the polynomial coefficients. The nonlinear least-squares fit would now involve ($m + 3$) parameters: ($m + 1$) polynomial coefficients, the horizontal activation energy E_H, and the vertical activation energy E_V. Note that in this case the estimates of two activation energies will be statistically correlated (23). This is to be contrasted with the estimation obtained from dynamic data from which the two activation energies are obtained independently and therefore uncorrelated.

In the present paper we extracted activation energies from the dynamic data and then used these activation energies to shift the steady-shear data and check whether steady-shear data superimpose. We could have done it another way; we could have extracted activation energies from steady shear data (as discussed above) and compared them with those extracted from dynamic data. We pursued the first approach because dynamic data are complete (include both the viscous and elastic response) and are more accurate than steady-shear data.

METHODOLOGY

The theory outlined in the previous section is applied practically as follows.

Step 0: Collect dynamic data measured at different temperatures. The larger the number of temperatures at which data is available and the wider the temperature range, the better the estimation of the activation energies will be.

Step 1: Perform a preliminary screening of the data. The plot of $\log_{10}(\tan\delta)$ vs. $\log_{10}(G^*)$ is particularly helpful.

- 1.1 If the data from different temperatures in the above plot of $\log_{10}(\tan\delta)$ vs. $\log_{10}(G^*)$ superimpose (within experimental error), then a vertical shift is not required and an $E_V = 0$ should be expected.
- 1.2 If the data from different temperatures in the plot of $\log_{10}(\tan\delta)$ vs. $\log_{10}(G^*)$ do not superimpose but fall onto parallel curves, then a vertical shift is required and a non-zero E_V should be expected.
- 1.3 If the data from different temperatures in the plot of $\log_{10}(\tan\delta)$ vs. $\log_{10}(G^*)$ do not superimpose and do not fall onto parallel curves, then we cannot handle this case within the present theoretical framework. Although rare, this case is indicative of relaxation times (or moduli) having non-uniform temperature dependence, and does occur in practice (e.g., certain multiphase systems).

Step 2: Calculate the horizontal and vertical activation energies, as described above. Examine the confidence intervals of the vertical activation energy and discard if found to be statistically insignificant (23).

Step 3: Using the computed activation energies, shift the raw data to a reference temperature for visual inspection of the goodness of superposition.

RESULTS AND DISCUSSION

Dynamic data (frequency response in the linear viscoelastic region) were obtained with the Rheometrics Mechanical Spectrometer (RMS) and the Rheometrics Dynamic Analyzer II (RDA2) operating in the parallel plate mode, while steady-shear viscosity data were obtained with a gas extrusion rheometer (25). All sample plaques for use in RMS and RDA2 were stabilized with additional antioxidants to avoid chain extension and scission during measurement.

Some of the data (HDPE-1 in *Table 1*, and LDPE-1 and LDPE-3 in *Table 5*) were obtained on solution dissolved samples. The polymer was dissolved in xylene, the xylene was allowed to evaporate, and the final sample was dried in vacuum for 72 h. Polymer samples were solution dissolved in order to eliminate effects of any shear prehistory (e.g., during pelletizing). Shear prehistory is known to affect the rheological behavior and its temperature dependence, especially for LDPE (17).

HDPE

Tabulated results for HDPE are given in *Table 1* for five different resins. In all cases the horizontal activation energy turns out to be about 6 kcal/mole, and the vertical activation energy is zero. The value of 0.8 kcal/mole for HDPE-1 must be treated with caution, due to the fact that the material was xylene dissolved. Also the value of 0.14 kcal/mole for HDPE-5 is marginally significant. These results are in accord with those of the literature (3).

LLDPE

Tabulated results for LLDPE are given in *Table 2*, for three different resins. The horizontal activation energy varies in the range 7 to 8 kcal/mole, which is

Table 1. Results for HDPE.

Resin	ρ g/cm^3	*MI*** g/10 min	E_H kcal/mole	E_V kcal/mole
HDPE-1*	0.96	1.0	6.60 ± 0.44	0.80 ± 0.33
HDPE-2	0.96	0.8	5.80 ± 0.52	0.0
HDPE-3	0.96	0.8	5.94 ± 0.58	0.0
HDPE-4	0.96	0.9	6.28 ± 0.49	0.0
HDPE-5	0.96	0.2	6.10 ± 0.22	0.14 ± 0.13

* = Xylene dissolved sample.
** = 190°C/2.16 Kg.

Table 2. Results for LLDPE.

Resin	Comonomer	*MI* g/10 min	ρ g/cm^3	E_H kcal/mole	E_V kcal/mole
LLDPE-1	Butene	1.0	0.918	7.27 ± 0.19	0.61 ± 0.14
LLDPE-2	Butene	1.0	0.918	7.07 ± 0.14	0.0
LLDPE-3	Octene	1.0	0.920	7.77 ± 0.24	0.25 ± 0.18

in agreement with literature results. The highest activation energy (7.77 kcal/mole) is for LLDPE-3, an octene based LLDPE (as opposed to LLDPE-1 and LLDPE-2, which are butene based LLDPEs). This result was expected since the activation energy increases with the molar volume of the repeating unit of the polymer (15).

The vertical activation energy is nearly zero for LLDPE-2 and LLDPE-3. For LLDPE-1 it is 0.61 kcal/mole, which represents a vertical shift factor of only 10% between 150 and 210°C.

As a typical example consider the LLDPE-1; a graph of $\log_{10}(\tan\delta)$ vs. $\log_{10}(G^*)$ is given in *Fig. 2*. Raw data of storage modulus and dynamic viscosity vs. frequency at different temperatures are plotted in *Fig. 3*. These same data upon shifting give the graph of *Fig. 4*. The good superposition is a verification that the activation energies used for the shifting (listed in *Table 2*, and in *Fig. 4*) are adequate.

Steady-shear data were also available for this material, and are plotted in *Fig. 5* (three temperatures) as shear stress vs. shear rate. Shifting these data (as explained earlier) gives the graph of *Fig. 6*, which shows good superposition, i.e. steady-shear data were superposed with the activation energies determined from linear viscoelastic data.

Polypropylene

Tabulated results for PP are given in *Table 3* for seven different resins. Averaging out the horizontal activation energies gives a value of 9.4 kcal/mole, again close to values reported in the literature (9–10 kcal/mole). The vertical activation energy turns out to be zero, or very small and marginally significant.

EVOH

Results for EVOH (ethylene–vinyl alcohol copolymer) are given in *Table 4* for two different resins. The average horizontal activation energy is 14.6 kcal/mole and the vertical activation energy is zero.

It is not clear why the vertical activation energy turns out to be zero, given that EVOH is produced

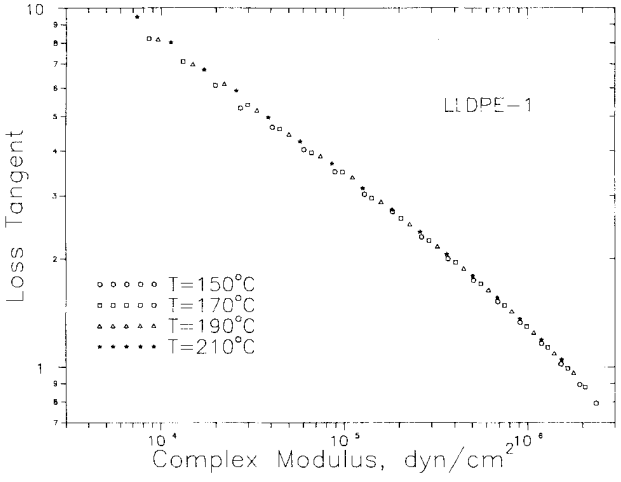

Fig. 2. Loss tangent vs. complex modulus data at different temperatures superimpose for a linear polyethylene (LLDPE-1).

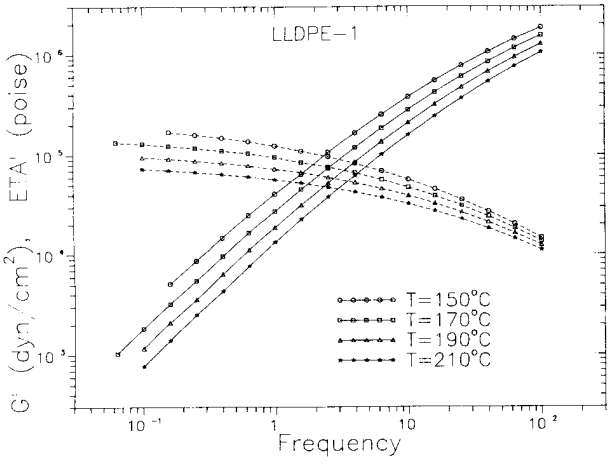

Fig. 3. Storage modulus and dynamic viscosity vs. frequency at different temperatures (LLDPE-1).

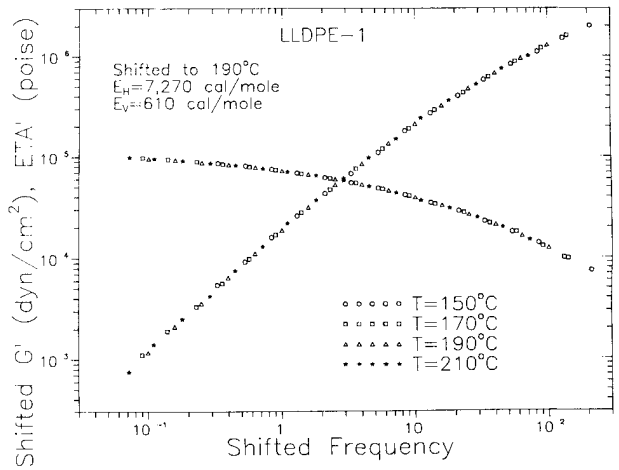

Fig. 4. Shifted data of storage modulus and dynamic viscosity vs. frequency, showing superposition (LLDPE-1).

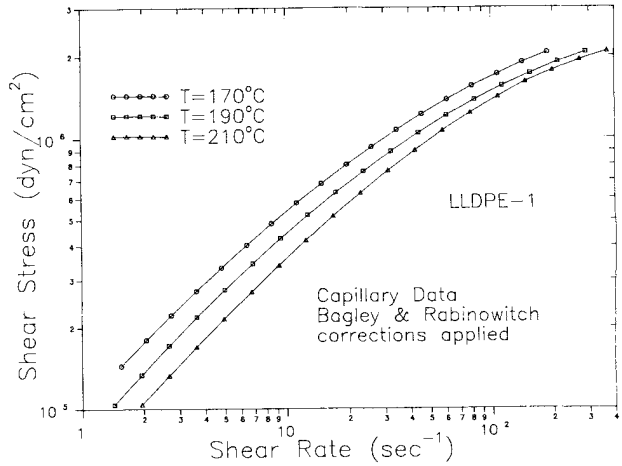

Fig. 5. Steady-shear data (shear stress vs. shear rate) at different temperatures (LLDPE-1).

through the hydrolysis of VAE (Vinyl acetate–Ethylene copolymer). VAE, in turn, does have long chain branching and does require a vertical shift. Part of the reason may be that all branches through the acetate group in VAE are lost after hydrolysis and, therefore, EVOH is expected to have substantially less long chain branching than its predecessor VAE (26). A second possible reason relates to the temperature coefficient of unperturbed chain dimensions $d\ln\langle r_o^2\rangle/dT$. As was pointed out by Graessley (12), "species where long branches have little effect on the temperature coefficient of viscosity also have small temperature coefficients of chain dimensions." For polyethylene this coefficient is $d\ln\langle r_o^2\rangle/dT = -1.1*10^{-3}\ °C^{-1}$ (12, 27, 28). Stars of polystyrene, polybutadiene, and polyisoprene have positive and small temperature coefficients of chain dimensions and do not show the anomalous behavior due to long chain branching as polyethylene does (12). Therefore, EVOH may have a value of $d\ln\langle r_o^2\rangle/dT$, such that the effect of long chain branches on the temperature dependence of rheology is minimal. More work on this matter is in progress.

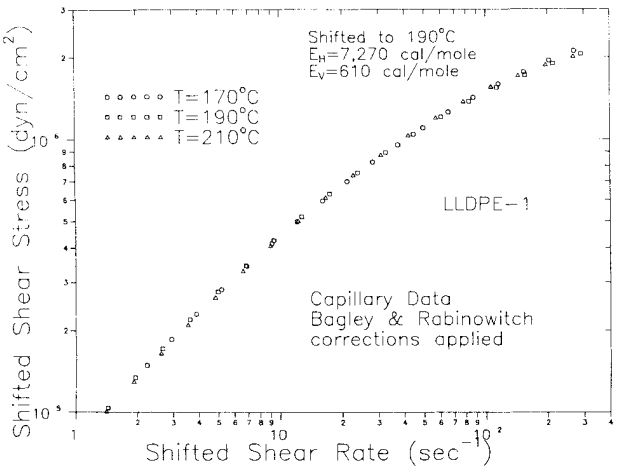

Fig. 6. The data of Fig. 5, shifted at 190°C (LLDPE-1).

Table 3. Results for Polypropylene.

Resin	Comments	*MFR** g/10 min	E_H kcal/mole	E_V kcal/mole
PP-1	Homopolymer	37	8.95 ± 0.23	0.29 ± 0.17
PP-2	Homopolymer	26	9.94 ± 0.32	0.24 ± 0.19
PP-3	Random Copolymer	2	8.74 ± 0.22	0.36 ± 0.16
PP-4	—	0.33	10.74 ± 0.22	0.0
PP-5	Homopolymer	42	8.79 ± 0.26	0.0
PP-6	Copolymer	0.2	9.90 ± 0.55	0.0
PP-7	Copolymer 25.9% $C_2^=$	13.4	8.51 ± 0.66	0.0

* = 230°C/2.16 Kg

Table 4. Results for EVOH.

Resin	Comments	*MI* g/10 min	E_H kcal/mole	E_V kcal/mole
EVOH-1	32% mole $C_2^=$ 1.19 g/cm³	1.3	15.45 ± 0.96	0.0
EVOH-2	44% mole $C_2^=$ 1.14 g/cm³	5.5	13.78 ± 0.60	0.0

LDPE

Results for LDPE (long chain branched) are tabulated in *Table 5*: invariably, the vertical activation energy is non-zero and around 2 kcal/mole (with the exception of the model star-HPBs).

Let us consider in some detail a typical LDPE—the LDPE-4. Raw data from different temperatures are plotted as $\log_{10}(\tan\delta)$ vs. $\log_{10}(G^*)$ in *Fig. 7*. Obviously the data do not superimpose, but they fall onto parallel curves, an indication that a vertical shift is the necessary and sufficient step to superpose the data. Indeed, the effect of vertical superposition is shown in *Fig. 8*. Now the data superimpose and they form a master curve. It is important to note that the two shifts (horizontal and vertical) are sufficient to superpose all viscoelastic properties. As is shown in *Fig. 11*, both the storage modulus vs. frequency data (*Fig. 9*) and loss modulus vs. frequency data (*Fig. 10*) superimpose after a horizontal and vertical shift are applied to the data.

The importance of the vertical shift will be further illustrated by examining the problems resulting from a horizontal-only shift. Traditionally, the data are shifted horizontally only. As was shown for HDPE, LLDPE, PP, and EVOH (and for a wide variety of other systems) a horizontal-only shift is adequate for linear materials. When we attempt to apply a horizontal-only shift for long chain branched materials we see the following: *Fig. 12* shows a horizontal-only shift for storage modulus vs. frequency data. The superposition is indeed good for the storage modulus data. This superposition was made possible by allowing the activation energy to become a function of storage modulus. Specifically, the requirement of a horizontal-only shift produces a set of temperature shift factors at every level of storage modulus, from which set of shift factors we compute an activation energy at every level of storage modulus.

When the temperature shift resulting from *Fig. 12* is applied to the loss modulus data we get *Fig. 13*, which shows that the data do not superimpose very well. (One must be very critical and demanding on the goodness of superposition. If the non-superposition of the data in *Fig. 13* is dismissed as simple scatter, then one would totally miss the problem. In fact this is what has happened in the literature, and it was pointed out earlier by Verser and Maxwell (19). Moreover, the activation energy required for shifting the data in *Fig. 12* is now a function of storage modulus, as shown in *Fig. 14* (solid line), decreasing with increasing modulus.

Similarly, when we apply a horizontal-only shift to the loss modulus data (by allowing the activation energy to become a function of loss modulus), we get good superposition for loss modulus as shown in *Fig. 15*. But applying this temperature shift to the

Table 5. Results for LDPE.

Resin	Comments	MI g/10 min	ρ g/cm^3	E_H kcal/mole	E_V kcal/mole
LDPE-1 (NBS 1476*)	Xylene Dissolved	—	0.931	14.67 ± 0.30	2.31 ± 0.26
LDPE-2 (NBS 1476)	Pellet	1.2	0.931	16.02 ± 0.38	2.47 ± 0.31
LDPE-3¶	Xylene Dissolved	—	0.919	15.27 ± 0.28	2.44 ± 0.17
LDPE-4¶	Pellets	1.1	0.919	16.01 ± 0.15	2.28 ± 0.09
LDPE-5	Pellets	2.9	0.926	15.78 ± 0.20	1.45 ± 0.13
LDPE-6	Pellets	1.8	0.923	14.62 ± 0.17	1.77 ± 0.13
3-Star HPB	M_w = 98,000 Data from (10)	—	—	15.31 ± 0.31	1.01 ± 0.32
4-Star HPB	M_w = 133,000 Data from (10)	—	—	16.47 ± 1.43	0.97 ± 0.37

* = Shift at constant modulus performed.
¶ = Same LDPE.

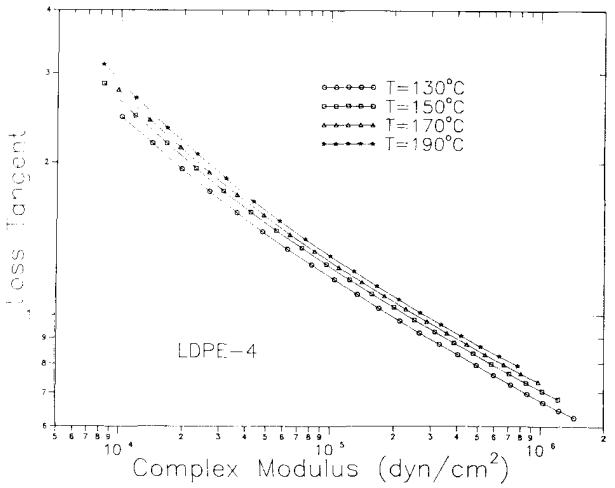

Fig. 7. Loss tangent vs. complex modulus data at different temperatures fall onto parallel curves for a long chain branched polyethylene (LDPE-4), illustrating the need for a modulus shift with temperature ("vertical" shift).

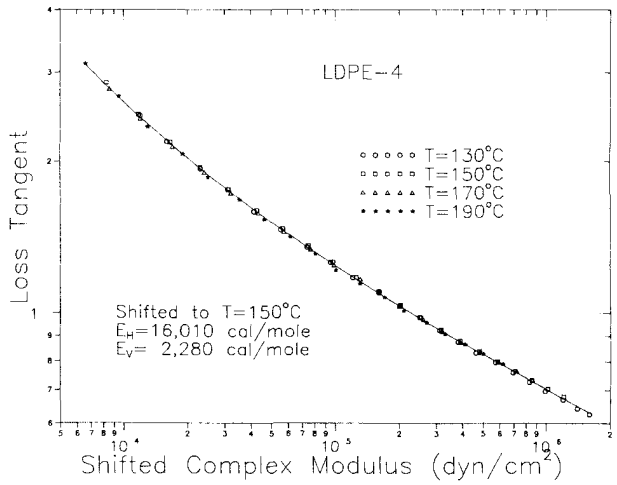

Fig. 8. The data of Fig. 7, superimpose after a "vertical" (modulus) shift has been applied to the data (LDPE-4).

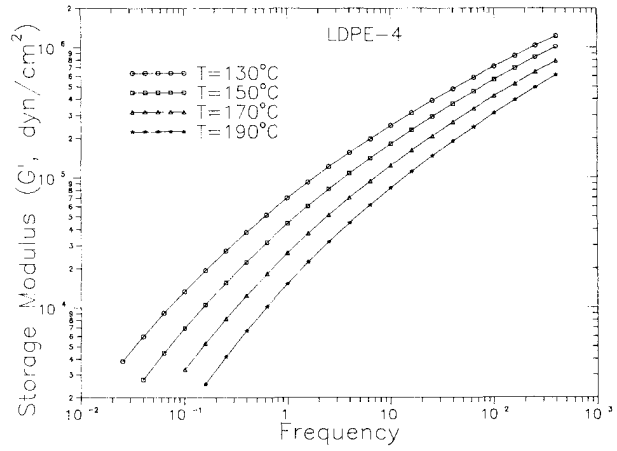

Fig. 9. Storage modulus vs. frequency at different temperatures (LDPE-4).

storage modulus data does not produce good superposition (*Fig. 16*). Also, the activation energy becomes a function of loss modulus (dashed line in *Fig. 14*).

Steady-shear data were also available for LDPE-4 at different temperatures, shown in *Fig. 17*. Applying a horizontal as well as a vertical shift to these data with activation energies determined from the dynamic data produces relatively good superposition, as shown in *Fig. 18*.

It should also be noted that comparison of results between LDPE-2 and LDPE-1 (pellet form and solution dissolved sample) and between LDPE-4 and LDPE-3 (pellet form and solution dissolved sample) shows only marginal differences (with regards to the temperature dependence). A more systematic study of the effect of shear prehistory on the temperature dependence of LDPE rheology is in progress and will be reported in a future paper.

As *Table 5* shows, all LDPEs require a vertical shift. There is a certain variation in the vertical activation energy E_V (e.g., compare values for LDPE-4, 5, 6), which one would expect to be related to long chain branching (LCB) parameters. *Figure 19* shows apparent (not corrected for branching) molecular weight distributions for three LDPEs from *Table 5*. For the

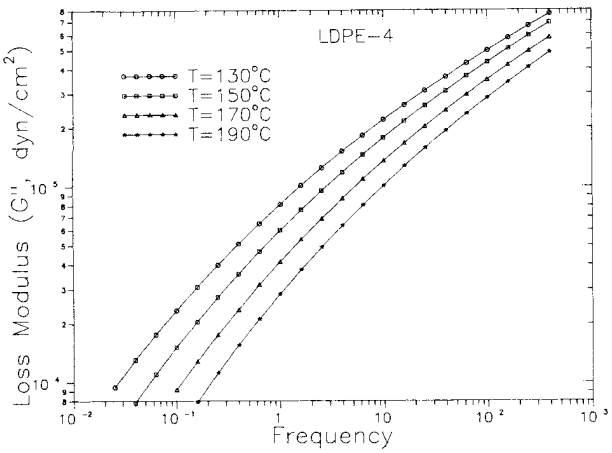

Fig. 10. Loss modulus vs. frequency at different temperatures (LDPE-4).

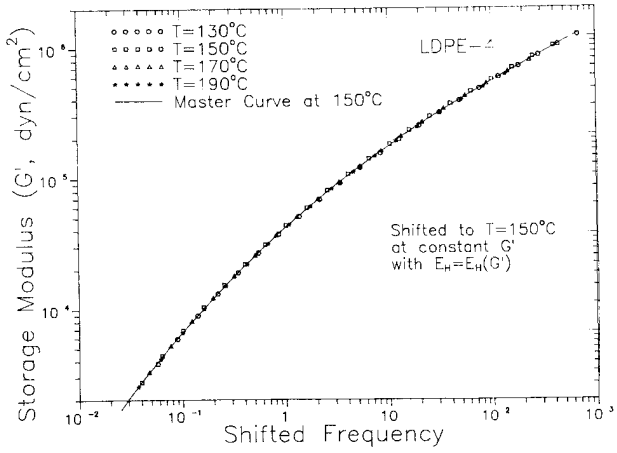

Fig. 12. The storage modulus data of Fig. 9 (LDPE-4), shifted horizontally only, with an activation energy as a function of storage modulus.

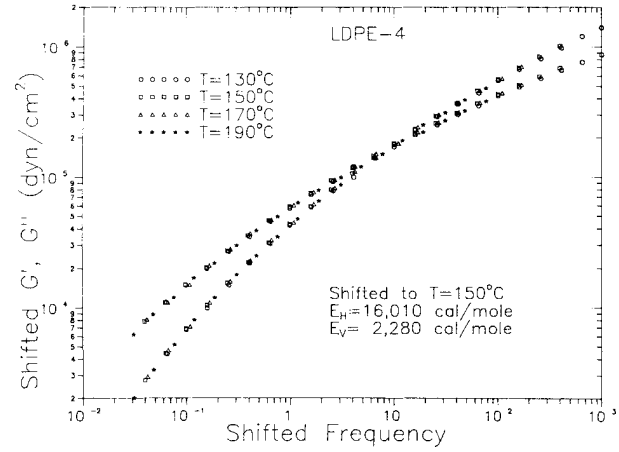

Fig. 11. The storage and loss modulus data of Figs. 9 and 10 after horizontal and vertical shifting, showing good superposition (LDPE-4).

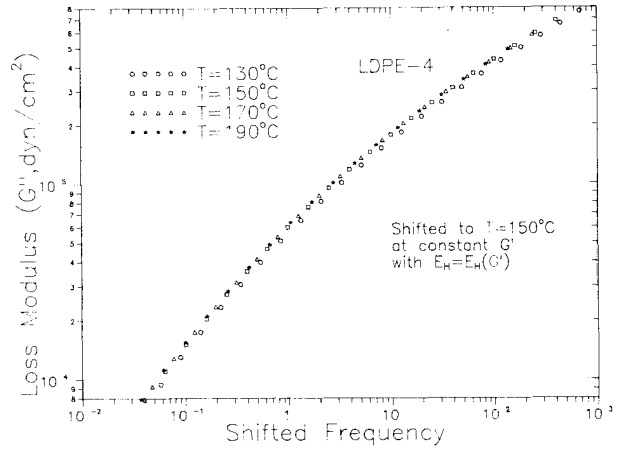

Fig. 13. The temperature shift from Fig. 12 applied to the loss modulus data (LDPE-4).

LDPEs in *Fig. 19* we expect an ordering in the level of LCB as LDPE-6/LDPE-5/LDPE-4, with LDPE-4 having the highest level of LCB. The E_V values of *Table 5* do not follow this order. One might expect a better correlation of E_V with other LCB parameters such as branch length and distribution. Unfortunately, this type of information was not available for the LDPEs studied in this work. It appears that the E_H and E_V values within the LDPE group of resins do not correlate with the level of LCB present in these resins.

It is interesting that even Graessley's model star-branched polybutadienes (10) show the necessity of a vertical shift (HPB in *Table 5*). In fact, Ref. 10 discussed the anomaly observed when shifting the data horizontally only (i.e., the modulus dependence of activation energy, see *Fig. 9* in Ref. 10). As was mentioned repeatedly above, a graph of $\log_{10}(\tan\delta)$ vs. $\log_{10}(G^*)$ can immediately identify the necessity (or absence thereof) of a vertical shift. The graph for the 3-star HPB in *Fig. 20* clearly shows parallel curves that require vertical shift.

Naturally, the question arises as to what makes long chain branched materials to require a vertical shift. One potential answer can be provided with reference to *Eq 11* and the concept of molecular weight between entanglements (suggested also by Graessley in his discussions of the effect of long chain branches on the rheology and polymer melts and its temperature sensitivity (11, 12)). For a vertical activation energy of 1.0 kcal/mole and greater, *Eq 11* predicts that the molecular weight between entanglements decreases with increasing temperature. This means that the entanglement density increases with increasing temperature, although it is not clear why would the entanglement density increase (with increasing temperature) for long chain branched and not for linear polymers.

As noted by Graessley (12), the temperature dependence of entanglement spacing is one of two contributing factors. The second relates to the suppression of reptation in branched polyethylenes (12). Linear chains rearrange by reptation; long chain

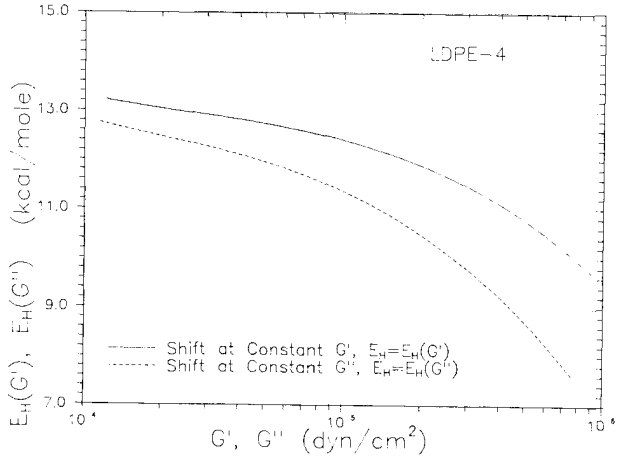

Fig. 14. Activation energy as a function of storage modulus (for horizontal-only shift at constant G') and as a function of loss modulus (for horizontal-only shift at constant G").

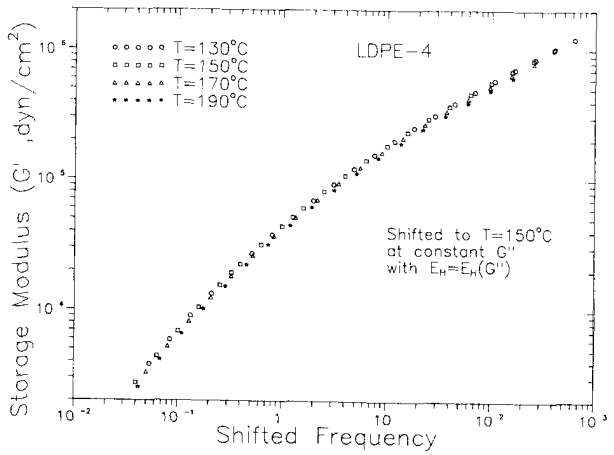

Fig. 16. The temperature shift from Fig. 15 applied to the storage modulus data (LDPE-4).

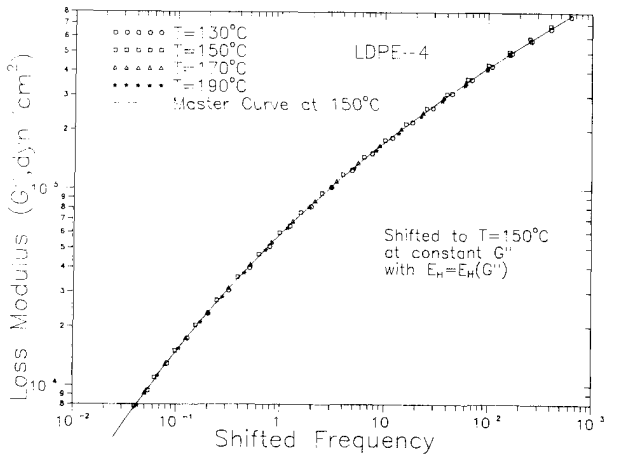

Fig. 15. The loss modulus data of Fig. 10 (LDPE-4), shifted horizontally only, with an activation energy as a function of loss modulus.

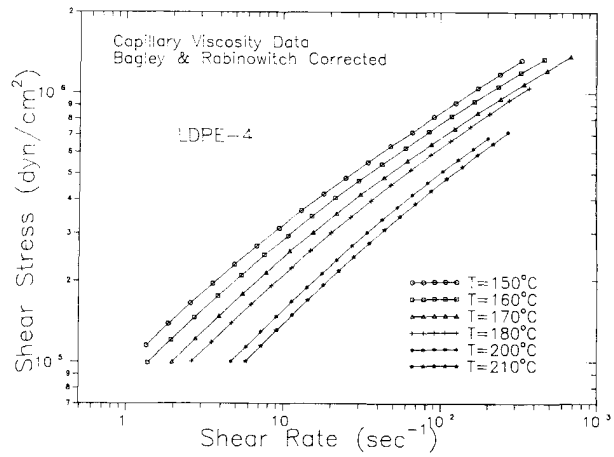

Fig. 17. Steady-shear data (shear stress vs. shear rate) at different temperatures (LDPE-4).

branches block reptation and rearrange by a process of "path breathing" (12). Both mechanisms have an impact on the temperature dependence of rheology, but it is not clear how to separate the two effects.

EVA

Results for EVA (ethylene–vinyl acetate copolymers) are tabulated in *Table 6* for two resins. The horizontal activation energy for EVA-1 is higher than that for EVA-2, presumably due to its higher VA content. As expected, a vertical activation energy of similar level as that of LDPE was found, thus further reconfirming that the necessity of the vertical shift is associated with long chain branching.

CONCLUDING REMARKS

The fundamentals of the temperature dependence of rheology were reviewed. We considered the case (by far the most common in polymer melts) where all relaxation times have the same temperature dependence (characterized by a "horizontal activation energy") and all relaxation moduli have the same temperature dependence (characterized by a "vertical activation energy"). Procedures were outlined for extracting these activation energies for rheological data. The recommended (and adopted) approach was to extract the temperature dependence from linear viscoelastic data; in this case the two activation energies can be estimated independently (and statistically uncorrelated).

It was also shown theoretically (and demonstrated experimentally) that neglect of the vertical shift leads to a stress (or modulus) dependent activation energy and makes impossible the superposition of both loss and storage modulus data. The long standing problem of a stress-dependent activation energy in long chain branched LDPE was identified as originating from the neglect of the vertical shift.

The theory was applied successfully to many polyolefin melts, including HDPE, LLDPE, PP, EVOH, LDPE, and EVA. Linear polymers (HDPE, LLDPE, PP) and EVOH do not require a vertical shift, but long

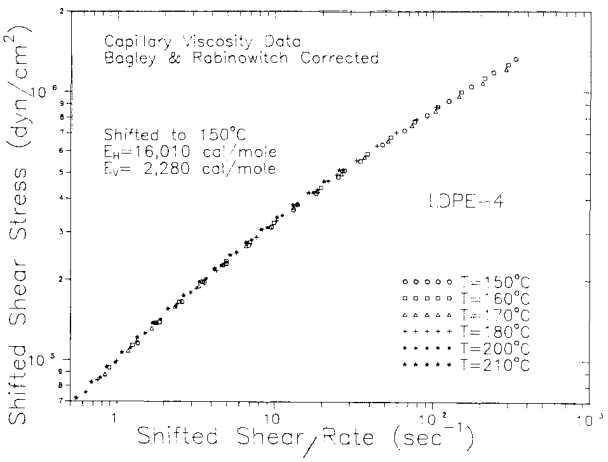

Fig. 18. The data of Fig. 17 shifted at 150°C, using the activation energies computed from dynamic data (LDPE-4).

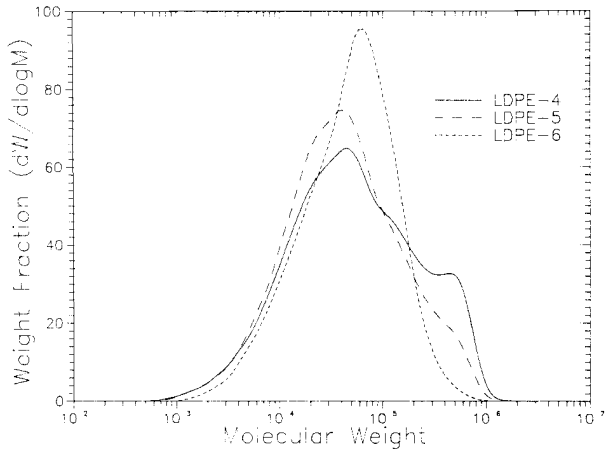

Fig. 19. Apparent Molecular Weight Distributions (uncorrected for long chain branching) for three LDPEs.

chain branched polymers do (LDPE, EVA). Steady-shear viscosity data can be superimposed using activation energies extracted from dynamic data.

APPENDIX: MELT INDEX SHIFT FOR EVA

As an example drawn from industrial practice, consider the Melt Index (MI) of a low %VA (vinyl acetate) EVA (ethylene–vinyl acetate) copolymer (e.g., 5% VA); it is measured at 2.16 Kg load at 190°C. Suppose we want to compare this resin with a high %VA EVA (e.g., 30% VA), which is characterized by a Melt Flow Rate (MFR) measured at 2.16 Kg load at 125°C (high %VA EVA degrades at high temperatures). We need to know what is the equivalent MFR of the low %VA EVA, or the equivalent MI of the high %VA EVA. It turns out that we can *estimate* the equivalent MI of the high %VA EVA, with the relation:

$$\text{MFR @ (2.16 Kg, 125°C)} = 0.116 * \text{MI @ (2.16 Kg, 190°C)}, \quad \text{for high \%VA EVA}$$

The above equation, whose derivation is considered

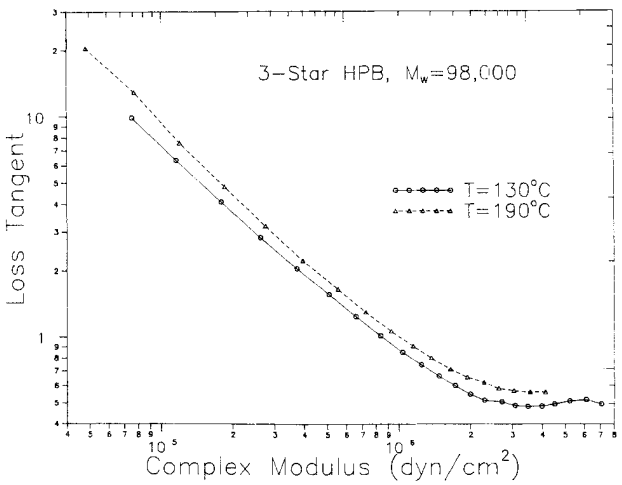

Fig. 20. Rheological data for 3-Star HPB (data from (10)).

Table 6. Results for EVA.

Resin	ρ g/cm³	MI g/10 min	Weight %VA	E_H kcal/mole	E_V kcal/mole
EVA-1	0.98	3.5	51	17.63 ± 0.30	1.65 ± 0.15
EVA-2	0.932	28	14.8	14.30 ± 0.53	2.04 ± 0.36

below, shows that a pre-established temperature dependence of rheology allows the prediction of rheological properties at one temperature given these properties at another temperature.

The Melt Index shift with temperature can be worked out by considering the temperature dependence of steady-shear data and the definition of the Melt Index. The Melt Index (MI) can be *approximately* computed from steady-shear data according to the equation:

$$\text{MI} = \frac{\dot{\gamma}}{2.4} \text{ at } \sigma = 1.95 \cdot 10^5 \text{ dyn/cm}^2 \qquad \text{(A.1)}$$

Note that the load specified in the MI (2.16 Kg) determines the stress σ. The temperature affects the shear rate, through the temperature dependence of viscosity.

The temperature dependence of steady-shear data was examined in §2.6, and it was quantified in *Eq 29*. For the purpose of the derivation to follow, we will assume that the shear stress vs. shear rate can be approximated by a power-law relationship, in the neighborhood of $\sigma = 1.95 * 10^5$ dyn/cm²:

$$\sigma = c_1 \cdot \dot{\gamma}^n \qquad \text{(A.2)}$$

where c_1 is a proportionality constant, known as the consistency index, and n is the power-law-index. To include the temperature dependence, *Eq A.2* must be written as:

$$b_T \cdot \sigma = c_1 \cdot (\alpha_T \cdot \dot{\gamma})^n \qquad \text{(A.3)}$$

where α_T and b_T are the horizontal and vertical shift factors defined in *Eqs 8* and *12* respectively. Combi-

nation of *Eqs A.1* and *A.3* gives:

$$MI(T) = \frac{b_T^{1/n}}{2.4\alpha_T}\left(\frac{\sigma}{c_1}\right)^n \qquad (A.4)$$

Taking the reference temperature T_o that appears in the definition of α_T and b_T to be 190°C, and using the fact that the stress σ is kept constant during melt index measurements at different temperatures, we derive the following from *Eq A.4*:

$$\frac{MI(T)}{MI(190°C)} = \frac{b_T^{1/n}}{\alpha_T} \qquad (A.5)$$

Equation A.5 can now be used to shift melt index with temperature. Application to high EVAs is considered below: from *Table 6*, we use $E_H = 14.9$ kcal/mole and $E_V = 1.97$ kcal/mole (estimated averages for the range 13 to 30% VA). Then the shift factors from 125 to 190°C are (substituting in *Eqs 8, 12*, $T = 125°C$, $T_o = 190°C$): $\alpha_T = 14.08$ and $b_T = 1.42$. For the power-law-index n we will use the value $1/n = 1.4$ at $\sigma = 1.95 * 10^5$ dyn/cm^2, determined from viscosity data on a series on EVA resins (the value $1/n = 1.4$ represents an average). Substituting the above shift factors and power-law-index into *Eq A.5* we get:

$$\frac{MI(125°C)}{MI(190°C)} = 0.116 \qquad (A.6)$$

Equation 6 is the equation used earlier in the introduction of this appendix. Comparison with experimental data is given in *Fig. A.1*; the line is *Eq A.6* and the symbols are experimental data; the comparison shows reasonable agreement.

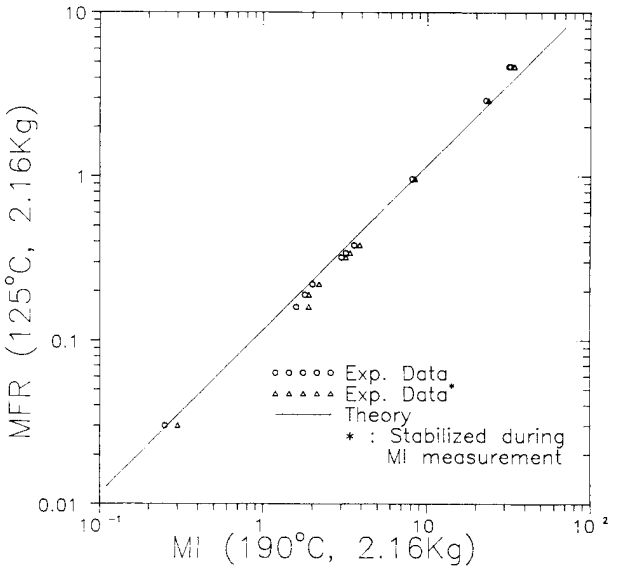

Fig. A.1. Comparison of theory and experiment for Melt Index shift with temperature for EVA (Ethylene–Vinyl Acetate copolymers).

ACKNOWLEDGMENT

The authors are indebted to Quantum Chemical Corp., USI Division for permission to publish this paper. Helpful comments by Dr. L. Wild are also acknowledged.

REFERENCES

1. C. D. Han and K.-W. Lem, *Polym. Eng. Rev.*, **2**, 135 (1982).
2. E. R. Harrell and N. Nakajima, *J. Appl. Polym. Sci.*, **29**, 995 (1984).
3. R. A. Mendelson, *Polym. Eng. Sci.*, **8**, 235 (1968).
4. H. Markovitz, *J. Polym. Sci.: Symp.* **No. 50**, 431 (1975).
5. A. J. Staverman and F. Schwarzl, in *Die Physik der Hochpolymeren*, Vol. 4, Ch. 1, H. A. Stuart, ed., Springer Verlag, Berlin (1956).
6. J. D. Ferry, *Viscoelastic Properties of Polymers*, Third Edition, J. Wiley, New York (1980).
7. R. Sabia, *J. Appl. Polym. Sci.*, **8**, 1651 (1964).
8. R. A. Mendelson, *SPE Trans.*, **5**, 34 (1964).
9. R. S. Porter, J. R. Knox, and J. F. Johnson, *Trans. Soc. Rheol.*, **12**, 409 (1968).
10. V. R. Raju, H. Rachapudy, and W. W. Graessley, *J. Polym. Sci.: Polym. Phys. Ed.*, **17**, 1223 (1979).
11. W. W. Graessley, *Acc. Chem. Res.*, **10**, 332 (1977).
12. W. W. Graessley, *Macromolecules*, **15**, 1164 (1982).
13. A. Santamaria, *Mater. Chem. Phys.*, **12**, 1 (1985).
14. R. S. Porter and J. F. Johnson, *J. Polym. Sci., Part C*, **15**, 365 (1966).
15. R. S. Porter and J. F. Johnson, *J. Polym. Sci., Part C*, **15**, 373 (1966).
16. M. S. Jacovic, D. Pollock, and R. S. Porter, *J. Appl. Polym. Sci.*, **23**, 517 (1979).
17. M. Rokudai and T. Fujiki, *J. Appl. Polym. Sci.*, **26**, 1343 (1981).
18. H. M. Laun, *Prog. Coll. Polym. Sci.*, **75**, 111 (1987).
19. D. W. Verser and B. Maxwell, *Polym. Eng. Sci.*, **10**, 122 (1970).
20. J. T. Gotro and W. W. Graessley, *Macromolecules*, **17**, 2767 (1984).
21. J. T. Gotro and W. W. Graessley, and L. J. Fetters, *Macromolecules*, **17**, 2775 (1984).
22. J. M. Carella, J. T. Gotro, and W. W. Graessley, *Macromolecules*, **19**, 659 (1986).
23. G. E. P. Box, W. G. Hunter, and J. S. Hunter, *Statistics for Experimenters*, J. Wiley, New York (1978).
24. B. W. Terry and K. Yang, *SPE J.*, **20** (6), 1 (1964).
25. R. N. Shroff and M. Shida, *J. Appl. Polym. Sci.*, **26**, 1847 (1981).
26. S. H. Agarwal, R. F. Jenkins, and R. S. Porter, *J. Appl. Polym. Sci.*, **27**, 113 (1982).
27. J. E. Mark, *Rubber Chem. Technol.*, **46**, 593 (1973).
28. P. J. Flory, *Statistical Mechanics of Chain Molecules*, Interscience, New York (1969).